



Speed Dependence of Atomic Stick-Slip Friction in Optimally Matched Experiments and Molecular Dynamics Simulations

Qunyang Li,¹ Yalin Dong,² Danny Perez,³ Ashlie Martini,² and Robert W. Carpick¹

¹*Department of Mechanical Engineering and Applied Mechanics, University of Pennsylvania, Philadelphia, Pennsylvania 19104, USA*

²*School of Mechanical Engineering, Purdue University, West Lafayette, Indiana 47907, USA*

³*Theoretical Division T-1, Los Alamos National Laboratory, Los Alamos, New Mexico 87545, USA*

(Received 17 September 2010; published 21 March 2011)

The atomic stick-slip behavior of a Pt tip sliding on a Au(111) surface is studied with atomic force microscopy (AFM) experiments and accelerated (i.e., reduced sliding speed) molecular dynamics (MD) simulations. The MD and AFM conditions are controlled to match, as closely as possible, the geometry and orientation, load, temperature, and compliance. We observe clear stick-slip without any damage. Comparison of both MD and AFM results with the thermally activated Prandtl-Tomlinson model shows that MD results at the highest speeds are not in the thermally activated regime. At lower speeds, within the thermally activated regime, AFM and MD provide consistent energetics, but attempt frequencies differ by orders of magnitude. Because this discrepancy lies in attempt frequencies and not energetics, atomistic details in MD simulations can be reliably used in interpreting AFM data if the MD speeds are slow enough.

DOI: [10.1103/PhysRevLett.106.126101](https://doi.org/10.1103/PhysRevLett.106.126101)

PACS numbers: 68.35.Af, 02.70.Ns, 46.55.+d, 62.20.Qp

Atomic stick-slip friction, where sliding surfaces stick and then slip with atomic periodicity, is a beautiful yet imperfectly understood phenomenon [1,2]. Atomic stick-slip friction involves instabilities caused by the downward gradient of the lateral tip-sample interaction force in the sliding direction approaching or exceeding the lateral stiffness of the system [3]. The characteristic repeating “sawtooth” pattern emerges if the lateral interaction is spatially periodic in systems with finite stiffness; this is referred to as the Prandtl-Tomlinson (PT) model [4,5]. The PT model with thermal activation (PTT model) predicts that friction increases nearly logarithmically with speed because at higher speeds there is less time per unit cell for thermally assisted hopping [6–8], a trend observed in several atomic force microscope (AFM) experiments. Atomic stick-slip behavior is also predicted by analytical models and molecular dynamics (MD) simulations [9], but direct comparison with experiment have been hindered by significant differences between model and experimental conditions. Here we present results from MD simulations and AFM where the materials, load, contact size, system compliance, temperature, crystallographic orientations, and sliding direction are identical within experimental uncertainty. Most crucially, the sliding speeds in the simulations are greatly reduced using accelerated MD [10], enabling measurements and simulations to be quantitatively compared within the same physical regime.

We choose to examine a platinum-coated tip sliding against a Au(111) surface [Fig. 1(a)]; these are both relatively inert materials with a large miscibility gap [11], inhibiting surface and interfacial chemical reactions. Au(111) surfaces were prepared by thermally evaporating gold onto freshly cleaved mica discs under high vacuum

followed by annealing with a hydrogen flame in air [12] resulting in unreconstructed (111) terraces [Fig. 1(a)], and then immediately transferred into a RHK-UHV 350 AFM. To desorb surface contaminants, films were heated to 400 °C for 5 minutes under vacuum (1×10^{-6} Torr). The chamber was then backfilled and continuously purged with the clean, dry nitrogen vapor from a liquid nitrogen dewar. All measurements were performed at room temperature with a Pt-coated silicon cantilever (AppNano). Transmission electron microscopy (TEM) images [Fig. 1(a)] show that the thermally evaporated Pt coating is polycrystalline; the tip end consists of a single nanocrystalline grain. The effective radius of curvature of the tip end is $R \approx 14$ nm according to the blind reconstruction technique [13]. The normal spring constant, $k_n = 0.13$ N/m, was calibrated using Sader’s method [14], and the optical sensitivity obtained from force-displacement measurements. Lateral forces were calibrated using the diamagnetic lateral force calibration method [15]. Unless otherwise noted, the normal load was kept constant at $F_n = 0.6$ nN, and the scan size at 5 nm (except for the two highest speeds where the scan sizes were 10 and 20 nm, respectively). Scanning speed was primarily varied by changing the scanning frequency.

Gold films were stable upon contact with the Pt tip; no sample damage was observed unless loads exceeded ~ 10 nN, at which point sudden increases in friction and adhesion occurred and regular stick-slip motion disappeared. Cold welding of the bimetallic interface was likely responsible for this [16,17]. While a few recent papers [16,18,19] report friction on metal surfaces, all using Si tips, no experimental papers report elastic stick-slip behavior for a metal tip in contact with a metal surface. The behavior of the Au-Pt contacts, supported

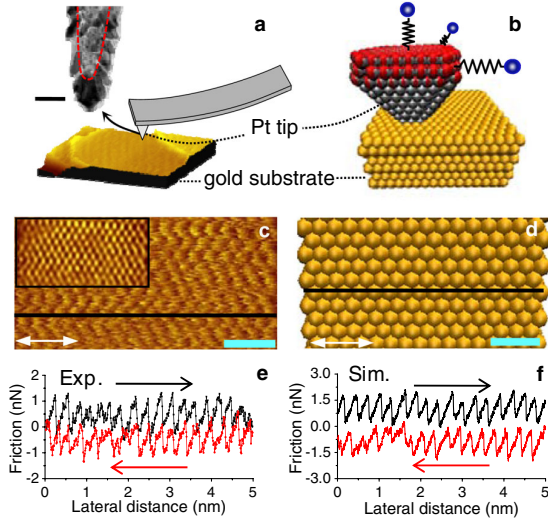


FIG. 1 (color online). (a) Schematic of the AFM experiment, and a $100 \times 100 \text{ nm}^2$ topographic AFM image of the Au(111) surface showing large terraces separated by monatomic steps. Inset above: TEM image of the Pt-coated probe. Scale bar is 20 nm. (b) Snapshot of the atomistic tip-substrate model. (c) Lateral force image on Au(111) at 0.6 nN load with a speed of 149 nm/s. Inset: Fourier low-pass filtered image. (d) Top view of the simulated Au(111) substrate. White arrows in (c),(d) denote the fast scanning direction. Scale bars are 1 nm. (e),(f) Variation of the experimental (e) and simulated (f) lateral force along the black horizontal line shown in (c) and (d), respectively. The simulation results in (f) are obtained for a relative surface orientation of 30° and a contact area of 7.32 nm^2 (91 atoms) under same normal load as in (c), and sliding speed 1 m/s.

by the MD simulation, indicates that stable metal-metal contact and sliding exists for these low-energy surfaces.

Typical lateral force images exhibit a clear threefold symmetric atomic stick-slip pattern with a period of $0.29 \pm 0.02 \text{ nm}$ [Fig. 1(c)], consistent with the 0.288 nm nearest-neighbor spacing of the Au(111) surface. The sliding direction, by design, is within 2.5° of the [110] direction [Fig. 1(c)]. The lateral force [Fig. 1(e)] shows the usual closed loop for sliding forward (black) and back (red). The “mean” and “peak” friction refer to half the difference between forward and backward sliding values for the average lateral force and the average local peak lateral forces, respectively. In this Letter, friction refers to mean friction unless otherwise specified.

For the simulations, the platinum tip was a truncated cone to mimic the presence of an oriented grain which is suggested by the TEM observations [Fig. 1(a)]. The tip was assumed to have a (111) termination (nearest-neighbor distance 0.277 nm), which is the lowest surface energy plane of Pt [Figs. 1(b) and 1(d)]. Because of the constraint of limited computational power, only the apex of the tip is modeled. The embedded atom method (EAM) was employed for all interatomic interactions [20]. The treatment is similar to the one we have reported for a Cu-Cu system [21]. Compliance of the cantilever and the upper body of the tip is modeled by coupling harmonic springs to the top

layers of the tip (as described in [22]). We prescribed the lateral spring stiffness in the model such that the resultant total lateral stiffness is consistent with that observed in the experiments ($\sim 6 \text{ N/m}$). The gold substrate, 2.2 nm thick and 5 nm wide, was subjected to periodic boundary conditions in the lateral direction. Simulations were run using parallel replica (ParRep) dynamics, an accelerated MD method that extends the time scale accessible to atomistic simulations of activated dynamics through a timewise parallelization strategy, enabling scanning speeds to be greatly reduced [10].

For the simulations, the tip and sample materials, applied load (0.6 nN), temperature (293 K), surface orientations, system compliance, and sliding direction were consistent with the experiments. The remaining parameters, i.e., contact area and tip rotation relative to the substrate, were optimized to match the experiments as illustrated in Figs. 2(a) and 2(b), respectively.

Contact area is at best measured indirectly in AFM [9] and thus extremely challenging to match with simulations. For all relative surface alignments, peak and average friction both increase as the contact area is increased. Therefore, we attribute the small but finite increase in peak friction with load observed experimentally ($\sim 0.4 \text{ nN}$ increase in friction over a 7 nN load range) to the increase in contact area resulting from elastic deformation of the tip and sample. We further assume that the peak friction is linearly proportional to the contact area through a constant friction shear stress, as seen in many experiments [9] and in simulations for incommensurate contacts [23]. We then fit the experimental peak friction vs normal load data with the Maugis-Dugdale continuum adhesive contact mechanics model [24] using the experimentally determined effective tip radius of 14 nm and the bulk elastic constants for gold ($E = 77.2 \text{ GPa}$, $\nu = 0.42$) and platinum ($E = 177 \text{ GPa}$, $\nu = 0.39$), giving a contact radius of $1.5 \pm 0.1 \text{ nm}$ ($7.1 \pm 0.6 \text{ nm}^2$ contact area) at 0.6 nN load. Based on this,

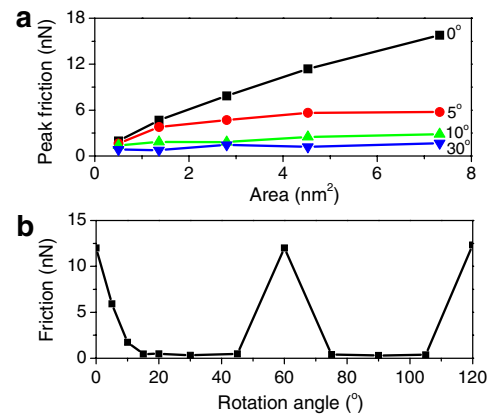


FIG. 2 (color online). (a) Peak friction vs contact area in the simulations for different relative orientations. In all cases, friction increases with contact area. (b) Mean friction force as a function of tip-substrate orientation for a load of 0.6 nN with a tip apex 91 atoms in size.

we selected the model tip of the closest size (7.32 nm^2 or 91 atoms). While this is a challenging aspect of matching experiment and simulation, errors in absolute friction values are likely minor since the dependences of friction on load in the experiment, and on area in the simulations of incommensurate contacts [Fig. 2(a)], are small.

Figure 2(b) illustrates the effect of relative tip-sample crystallographic orientation. Because of their close lattice constants, friction is large when the close-packed $\langle 100 \rangle$ directions of the tip and sample are aligned, but falls by ~ 10 when they are not aligned, consistent with the expected effect of commensurability [25]. It is not possible to determine the atomic structure of our Pt tip's surface experimentally, but the two surfaces are very likely misaligned since the Pt tip does not necessarily have a perfectly flat (111) orientation, and high friction is the exception in the simulations, only occurring for a very limited range of relative orientations. As friction is only weakly dependent on orientation in that regime, we select a mismatch angle of 30° as a representative value.

We prescribed the lateral spring stiffness in the model to be $\sim 6 \text{ N/m}$, matching the value of the total experimental lateral stiffness determined from the slope of the friction trace during the “stick” phase [Figs. 1(e) and 1(f)].

The speed dependence of mean friction is shown in Fig. 3. The gap between the AFM and MD scanning speeds, while substantial (a factor of ~ 5000), is orders of magnitude smaller than any previous work, allowing us to explore whether results are consistent between the two methods. Single stick-slip is clearly resolved under all conditions. We consider the predictions from the PTT model in the quasistatic, single slip regime [6–8,19,26]. Mean friction F_L is related to speed v through the nonlinear implicit equation [6]

$$\frac{1}{\beta k_B T} (F_c - F_L)^{3/2} = \ln \frac{v_0}{v} - \frac{1}{2} \ln \left(1 - \frac{F_L}{F_c} \right), \quad (1)$$

where T is the temperature, k_B is Boltzmann's constant, F_c the mean friction force at zero temperature, β a parameter determined by the shape of the lateral potential profile, and v_0 is a characteristic speed given by $v_0 = (2f_0\beta k_B T)/(3k_{\text{tot}}\sqrt{F_c})$, where f_0 is the characteristic attempt frequency, and k_{tot} the total lateral stiffness [6,26]. For a sinusoidal potential with periodicity a and barrier height E_0 , $F_c = \pi E_0/a$ and $\beta = 3\pi\sqrt{F_c}/(2\sqrt{2}a)$. Well below v_0 , friction increases nearly logarithmically with speed because the tip has less time and thus fewer opportunities to use thermal energy to overcome the local energy barrier to slip. Well above v_0 , thermal energy will not assist slip anymore, and friction approaches the plateau value of F_c . Several AFM experiments are consistent with Eq. (1) [6,7,18,26]. Furthermore, the statistical distribution of friction forces was measured to match predictions from the PTT model [8]. These results provide strong evidence that atomic stick-slip in AFM is attributable to thermally activated slip out of a local minimum as described by the PTT model.

Within the experimental range of speeds, 1 to 1000 nm/s, friction followed the low speed trend very well (cf. Fig. 3). With the fit parameters ($F_c = 0.55 \text{ nN}$, $\beta = 3.0 \times 10^5 \text{ N}^{3/2}/\text{J}$, and $f_0 = 49 \text{ kHz}$), the PTT model predicts that friction reaches the plateau at $\sim 10 \mu\text{m/s}$. While a fit to the PTT model is somewhat underconstrained without a direct observation of the force plateau, significantly postponing its onset would imply a drastic increase of f_0 into the tens of MHz, which is difficult to rationalize both in terms of low-frequency torsional modes of the cantilever (observed in other AFM measurements [6,26]) or in terms of apex bending modes (which are expected to be in the GHz [27]).

Using ParRep simulations, we numerically probed speeds from 5×10^6 to $2 \times 10^9 \text{ nm/s}$ (Fig. 3). Friction at higher speeds ($> 10^8 \text{ nm/s}$) clearly deviates from the trend expected for thermally activated sliding. This behavior is mostly determined by dissipative athermal dynamical processes, so the sliding is not governed by thermally activated stick-slip. Thermally activated stick-slip friction is only seen in MD at sufficiently low speeds, which are so far only achievable through accelerated MD. This severely limits the regime of validity of comparisons MD simulations to AFM experiments, because the AFM experiments are in a fundamentally different regime of sliding. This important limitation has been discussed only recently in the case of grain boundary sliding [28].

We estimate the high-speed limit F_c through molecular statics by finding the force required to cause a slip instability without the assistance of thermal activation. This additional calculation of F_c is used to constrain the fit of the MD results to the PTT model's prediction, yielding $F_c = 0.85 \text{ nN}$, $\beta = 3.6 \times 10^5 \text{ N}^{3/2}/\text{J}$, and $f_0 = 40 \text{ GHz}$. Both F_c and β are remarkably consistent with those from

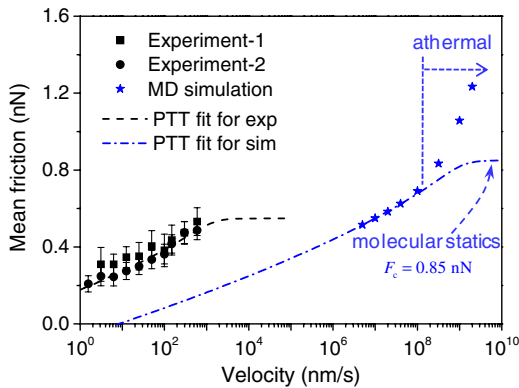


FIG. 3 (color online). Mean friction measured experimentally in two different runs (black squares, black circles) for speeds between 1 and 1000 nm/s, and predicted via accelerated MD (blue stars) for speeds between 0.005 m/s to 2 m/s. The black dashed curve and blue dash-dotted curve are fittings with the PTT model [6,7] for experimental and simulation data, respectively. The fit to the MD data uses $F_c = 0.85 \text{ nN}$ as obtained from molecular statics, and is only fit to data at speeds below 0.1 m/s; higher speeds cannot be fit to the curve due to athermal dissipative contributions to friction.

the experiment. The modest difference in F_c can be attributed to a slight overestimation of the contact area or to differences in relative tip-sample orientation angle. This agreement is consistent with previous observations that the main features of the energetics of the stick-slip process can be captured by fully atomistic, or even effective low-dimensional, models [29].

The discrepancy between the MD and AFM results lies in the attempt frequency. This difference, being unrelated to energetic aspects, cannot be attributed to elastic or plastic effects. Experimentally, the activation of a slip usually involves the motion of both the tip and cantilever; the slip rate prefactor is thus coupled to the low-frequency mechanical response of the apparatus, which extends down to the range of kHz. However, due to computational limitations inherent to fully atomistic methods, MD models explicitly contain only a limited number of atoms from the tip and substrate; the cantilever's compliance is instead introduced through effective springs, but its colossal inertia is usually ignored. While this rather aggressive coarse-graining procedure is adequate in terms of energetics, it fails to reproduce the richness of the mechanical response of the cantilever, in particular, with respect to low frequencies that are effectively raised from kHz up to GHz because of the small effective mass of the cantilever in the simulations, leading to artificially high attempt frequencies. In principle, this can be alleviated by reintroducing the inertia of the cantilever in an effective fashion, but only if driven at very low speeds ($< 10^4$ nm/s) to avoid exciting spurious resonances. This is a challenging task even when relying on accelerated MD algorithms [29]. Direct comparison with experiment is more likely to be achieved by fully parametrizing a rate theory approach from a representation of the AFM experiment that is either atomistic, in the manner of Perez *et al.* [30], or multiscale. This is promising because it allows the full atomistic details provided in MD simulations, particularly at the sliding interface, to be used in interpreting experimental stick-slip phenomena.

In conclusion, optimally matched experiments and accelerated MD simulations of atomic stick-slip friction for Pt tips on the Au(111) surface show that atomic stick-slip is thermally activated at low speeds. The consistent comparison was not possible with conventional MD as the high speeds lead to dynamic athermal effects not described by thermal activation. Remarkably similar parameters for the energy barrier and effective potential shape based on fitting the PTT model to the experiments and simulations are found for the thermally activated regime. Disparity still exists in the mean friction values due to the vastly different effective masses, and hence slip-attempt frequencies, in the two systems. However, because this discrepancy lies in attempt frequencies and not energetics, the rich atomistic details in MD simulations at slow speeds can indeed be reliably used in interpreting AFM data.

This work was funded by the National Science Foundation under Grants No. CMMI-0758604 &

0800154. Work at Los Alamos National Laboratory (LANL) was supported by the United States Department of Energy, Office of Basic Energy Sciences, Materials Sciences and Engineering Division. LANL is operated by Los Alamos National Security, LLC, for the National Nuclear Security Administration of the U.S. DOE under Contract No. DE-AC52-06NA25396. We thank A. F. Voter, M. Müser, and R. Bennewitz for useful discussions.

-
- [1] C. M. Mate *et al.*, *Phys. Rev. Lett.* **59**, 1942 (1987).
 - [2] S. Morita, S. Fujisawa, and Y. Sugawara, *Surf. Sci. Rep.* **23**, 1 (1996).
 - [3] G. M. McClelland, in *Adhesion and Friction*, edited by M. Grunze and H. J. Kreuzer, Springer Series in Surface Sciences Vol. 17 (Springer-Verlag, Berlin, 1990), p. 1.
 - [4] L. Prandtl, *Z. Angew. Math. Mech.* **8**, 85 (1928).
 - [5] G. A. Tomlinson, *Philos. Mag., Ser. 7*, **7**, 905 (1929).
 - [6] E. Riedo *et al.*, *Phys. Rev. Lett.* **91**, 084502 (2003).
 - [7] Y. Sang, M. Dube, and M. Grant, *Phys. Rev. Lett.* **87**, 174301 (2001).
 - [8] A. Schirmeisen, L. Jansen, and H. Fuchs, *Phys. Rev. B* **71**, 7 (2005).
 - [9] I. Szlufarska, M. Chandross, and R. W. Carpick, *J. Phys. D* **41**, 123001 (2008).
 - [10] A. F. Voter, *Phys. Rev. B* **57**, R13985 (1998).
 - [11] M. Hansen, *Constitution of Binary Alloys* (McGraw-Hill, New York, 1958).
 - [12] C. Noguez and M. Wanunu, *Surf. Sci.* **573**, L383 (2004).
 - [13] S. Dongmo *et al.*, *J. Vac. Sci. Technol. B* **14**, 1552 (1996).
 - [14] J. E. Sader, J. W. M. Chon, and P. Mulvaney, *Rev. Sci. Instrum.* **70**, 3967 (1999).
 - [15] Q. Li, K. S. Kim, and A. Rydberg, *Rev. Sci. Instrum.* **77**, 065105 (2006).
 - [16] N. N. Gosvami *et al.*, *Tribol. Lett.* **39**, 19 (2010).
 - [17] U. Landman *et al.*, *Science* **248**, 454 (1990).
 - [18] R. Bennewitz *et al.*, *Tribol. Lett.* **10**, 51 (2001).
 - [19] R. Bennewitz *et al.*, *Phys. Rev. B* **60**, R11301 (1999).
 - [20] A. F. Voter, Los Alamos National Laboratory technical Report No. LA-UR-93-3901 1993. For Au-Pt interactions, the EAM electron density function was rescaled to identify a single summed electron density for fcc Pt and Au. An arithmetic mean of the pure material potentials applied to model interactions between dissimilar atoms; A. F. Voter (private communication).
 - [21] A. Martini *et al.*, *Tribol. Lett.* **36**, 63 (2009).
 - [22] Y. L. Dong *et al.*, *Tribol. Lett.* (in press).
 - [23] B. Luan and M. O. Robbins, *Phys. Rev. E* **74**, 026111 (2006).
 - [24] D. Maugis, *J. Colloid Interface Sci.* **150**, 243 (1992).
 - [25] M. Dienwiebel *et al.*, *Phys. Rev. Lett.* **92**, 126101 (2004).
 - [26] E. Gnecco *et al.*, *Phys. Rev. Lett.* **84**, 1172 (2000).
 - [27] S. Y. Krylov *et al.*, *Phys. Rev. Lett.* **97**, 166103 (2006).
 - [28] Y. Mishin *et al.*, *Phys. Rev. B* **75**, 224101 (2007).
 - [29] D. Perez *et al.*, *Annual Reports in Computational Chemistry*, Accelerated Molecular Dynamics Methods: Introduction and Recent Developments Vol. 5 (Elsevier, New York, 2009), pp. 79.
 - [30] D. Perez *et al.*, *Phys. Rev. B* **81**, 245415 (2010).